

UCSF

UC San Francisco Previously Published Works

Title

Polymerase independent repression of FoxO1 transcription by sequence-specific PARP1 binding to FoxO1 promoter

Permalink

<https://escholarship.org/uc/item/7x54111m>

Journal

Cell Death & Disease, 11(1)

ISSN

2041-4889

Authors

Tian, Yu-Nan

Chen, Hua-Dong

Tian, Chang-Qing

et al.

Publication Date

2020

DOI

10.1038/s41419-020-2265-y

Peer reviewed

ARTICLE

Open Access

Polymerase independent repression of *FoxO1* transcription by sequence-specific PARP1 binding to *FoxO1* promoter

Yu-Nan Tian^{1,2}, Hua-Dong Chen^{1,2}, Chang-Qing Tian^{1,2}, Ying-Qing Wang^{1,2} and Ze-Hong Miao^{1,2,3}

Abstract

Poly(ADP-ribose) polymerase 1 (PARP1) regulates gene transcription in addition to functioning as a DNA repair factor. Forkhead box O1 (FoxO1) is a transcription factor involved in extensive biological processes. Here, we report that PARP1 binds to two separate motifs on the *FoxO1* promoter and represses its transcription in a polymerase-independent manner. Using *PARP1*-knock out (KO) cells, wild-type-*PARP1*-complemented cells and catalytic mutant *PARP1*^{E988K}-reconstituted cells, we investigated transcriptional regulation by PARP1. *PARP1* loss led to reduced DNA damage response and ~362-fold resistance to five PARP inhibitors (PARPis) in Ewing sarcoma cells. RNA sequencing showed 492 differentially expressed genes in a *PARP1*-KO subline, in which the *FoxO1* mRNA levels increased up to more than five times. The change in the FoxO1 expression was confirmed at both mRNA and protein levels in different *PARP1*-KO and complemented cells. Moreover, exogenous *PARP1* overexpression reduced the endogenous FoxO1 protein in RD-ES cells. Competitive EMSA and ChIP assays revealed that PARP1 specifically bound to the *FoxO1* promoter. DNase I footprinting, mutation analyses, and DNA pulldown FREP assays showed that PARP1 bound to two particular nucleotide sequences separately located at -813 to -826 bp and -1805 to -1828 bp regions on the *FoxO1* promoter. Either the PARPi olaparib or the *PARP1* catalytic mutation (E988K) did not impair the repression of PARP1 on the *FoxO1* expression. Exogenous *FoxO1* overexpression did not impair cellular PARPi sensitivity. These findings demonstrate a new PARP1-gene promoter binding mode and a new transcriptional *FoxO1* gene repressor.

Introduction

Poly(ADP-ribose) polymerase 1 (PARP1) plays critical roles in DNA repair *via* catalyzing the transfer of the ADP-ribosyl group of NAD⁺ onto acceptor proteins (including PARP1 itself) to form poly(ADP-ribose) polymers, a process known as poly(ADP-ribosylation) (PARylation)^{1–3}. PARP1 inhibitors (PARPis) have been shown to selectively kill homologous recombination repair

(HRR) deficient cancer cells^{1–3} by increasing PARP1-DNA binding due to suppression of autoPARylation of PARP1 on DNA⁴. Four PARPis (olaparib, rucaparib, niraparib, and talazoparib) have been clinically used for cancer therapy, and more are undergoing clinical or preclinical tests^{3,5–11}. Our recent studies have revealed that treatments of cancer cells with PARPis reduce the expression of 53BP1 or enhance the expression of COX-2, BIRC3, and SAMHD1, which contributes to cellular drug resistance^{12,13}. These findings suggest that transcriptional regulation by PARP1 appears to affect the cellular sensitivity to PARPis or other anticancer drugs. Down-regulation of *BRCA2* expression by PARP1 in an enzymatic activity dependent manner¹⁴ provides an additional supporting clue for this.

Correspondence: Ying-Qing Wang (yqwang@simm.ac.cn) or Ze-Hong Miao (zhmiao@simm.ac.cn)

¹Division of Anti-Tumor Pharmacology, State Key Laboratory of Drug Research, Shanghai Institute of Materia Medica, Chinese Academy of Sciences, Shanghai 201203, China

²University of Chinese Academy of Sciences, No.19A Yuquan Road, Beijing 100049, China

Full list of author information is available at the end of the article.

Edited by R. Mantovani

© The Author(s) 2020



Open Access This article is licensed under a Creative Commons Attribution 4.0 International License, which permits use, sharing, adaptation, distribution and reproduction in any medium or format, as long as you give appropriate credit to the original author(s) and the source, provide a link to the Creative Commons license, and indicate if changes were made. The images or other third party material in this article are included in the article's Creative Commons license, unless indicated otherwise in a credit line to the material. If material is not included in the article's Creative Commons license and your intended use is not permitted by statutory regulation or exceeds the permitted use, you will need to obtain permission directly from the copyright holder. To view a copy of this license, visit <http://creativecommons.org/licenses/by/4.0/>.

PARP1 has been reported to regulate gene transcription in several ways^{15–18}. The transcriptional regulation by PARP1 is dependent on or independent of its polymerase activity and varies in gene-, cell type-, and context-specific manners^{15,16}. All these indicate that the PARP1-mediated transcriptional regulation is complicated and unpredictable based on present knowledge. Therefore, further investigations, such as its DNA sequence dependency and its correlations with cellular PARPi sensitivity, are required.

We previously established *PARP1*-KO sublines of Ewing sarcoma RD-ES and SK-ES-1 cell lines, which were denoted as RD/KO1, RD/KO2, SK/KO1, and SK/KO2 separately⁴. Here, we first characterized these sublines about their responses to PARPis. Then, we conducted RNA profiling in both RD-ES and RD/KO1 cells to find changes in mRNA levels due to *PARP1* loss. Following a series of analyses and verifications, Forkhead box O1 (*FoxO1*) was selected for further explorations because the *PARP1* KO significantly increases its mRNA and protein levels in different cell lines, which was partly reversed by *PARP1* complementation. Subsequently, we demonstrated by electrophoretic mobility shift (EMSA) and chromatin immunoprecipitation (ChIP) that PARP1 binds to the *FoxO1* promoter. This binding was further confirmed to be DNA sequence specific by DNase I footprinting assays, EMSA, and flanking restriction enhanced pulldown (FREP) assays. Finally, the transcriptional inhibition of *FoxO1* by PARP1 was shown to be independent of its enzymatic activity and cellular PARPi sensitivity.

Results

Characterization of *PARP1*-knockout variants of RD-ES and SK-ES-1 cells

Ewing sarcoma is the fifth highest PARP1-expressing malignancy¹⁹. To investigate the transcriptional regulation by PARP1, we used cellular models generated from Ewing sarcoma RD-ES and SK-ES-1 cells by knocking out the *PARP1* gene, denoted as RD/KO1, RD/KO2, SK/KO1, and SK/KO2⁴. All these clones almost completely lost their PARP1 expression and PAR formation (Fig. 1a) and displayed ~362-fold resistance to five PARPis⁴. The treatment with PARPi olaparib led to apparently less increase in levels of γ H2AX [a marker of DNA double-strand breaks (DSB)]²⁰ in the *PARP1*-deficient cells than in their respective parental cells (Fig. 1b). The levels of central components involved in DNA damage response (DDR) such as RPA32, RAD51, CHK1, and CHK2 in both RD/KO1 cells and CRISPR-mediated *PARP1* KO (Cri/KO) cells were similar to that of the parent RD-ES cells and the wild-type-*PARP1*-complemented RD/KO1 (RD/KO1-WT) cells⁴ (Fig. 1c). Notably, complementation with WT-*PARP1* only partially restored PARPi sensitivity in RD/KO1-WT cells (Fig. 1d).

Depletion of *PARP1* increases *FoxO1* expression

To identify target genes transcriptionally regulated by PARP1, we conducted transcription profiling in RD/KO1 cells and parental cells by RNA-seq. The results showed that the expression of 492 genes changed significantly in *PARP1*/KO cells [\log_2 fold change >1 with statistical significance ($p < 0.05$)]. The volcano plot (Fig. 1e) and the hierarchical clustered heatmap (Fig. 1f) revealed that among these expression-changed genes, 277 genes were upregulated, and 215 genes were downregulated (These genes in hierarchical clustered heatmap were shown in Supplementary Table S1 from top to bottom.) Among them, KEGG analysis further demonstrated that 23 genes were involved in “pathways in cancer” while the GO analysis indicated that 20 genes participated in “regulation of sequence-specific DNA binding transcription factor activity.” Interestingly, 10 genes were common to both (Fig. 1g). Among the 10 genes, the expression of seven genes changed obviously (\log_2 fold change >2), including TNF alpha induced protein 3 (*TNFAIP3*; up), nuclear factor kappa B subunit 2 (*NF- κ B2*; up), nuclear factor kappa B subunit 1 (*NF- κ B1*; up), NF- κ B inhibitor alpha (*NF- κ BIA*, also known as *I κ B α* ; up), *FoxO1* (up), inhibitor of nuclear factor kappa B kinase subunit beta (*I κ BKB*; down), and androgen receptor (*AR*; down) (Supplementary Table S2).

PARP1 has been reported to support the transcriptional function of AR¹⁷. Additionally, the above results show that genes related to NF- κ B1 signaling might be affected most due to *PARP1* loss. Thus, to verify the results from the transcription profiling, we used parental cells (RD-ES and SK-ES-1), *PARP1*-KO cells (RD/KO1 and SK/KO1), and their WT-*PARP1*-complemented cells (RD/KO1-WT and SK/KO1-WT)⁴. RT-qPCR revealed that though the mRNA levels of *TNFAIP3*, *I κ B α* , and *NF- κ B1* were strikingly elevated due to *PARP1* loss, complementation with WT-*PARP1* did not reduce their elevation (Fig. 2a). Moreover, western blotting further showed that *PARP1* loss caused increased TNFAIP3 protein levels but no change in *I κ B α* or *NF- κ B1* levels. In addition, *PARP1* reconstitution led to no (*I κ B α* or *NF- κ B1*) or only weak (*TNFAIP3*) changes at the protein levels (Fig. 2b). These inconsistent results indicated that genes related to NF- κ B1 signaling might not be regulated by PARP1, at least not in detected Ewing sarcoma cells.

Therefore, we turned to *FoxO1*, which encodes a transcription factor that regulates gene expression, controlling various cellular processes²¹. For changes in *FoxO1* gene expression caused by either *PARP1* loss or complementation in different cells, both RT-qPCR and western blotting provided consistent results to the transcription profiling (Fig. 2c and Supplementary Table S1). RNA-seq revealed increased *FoxO1* mRNA levels up to more than five times in RD/KO1 cells (Supplementary

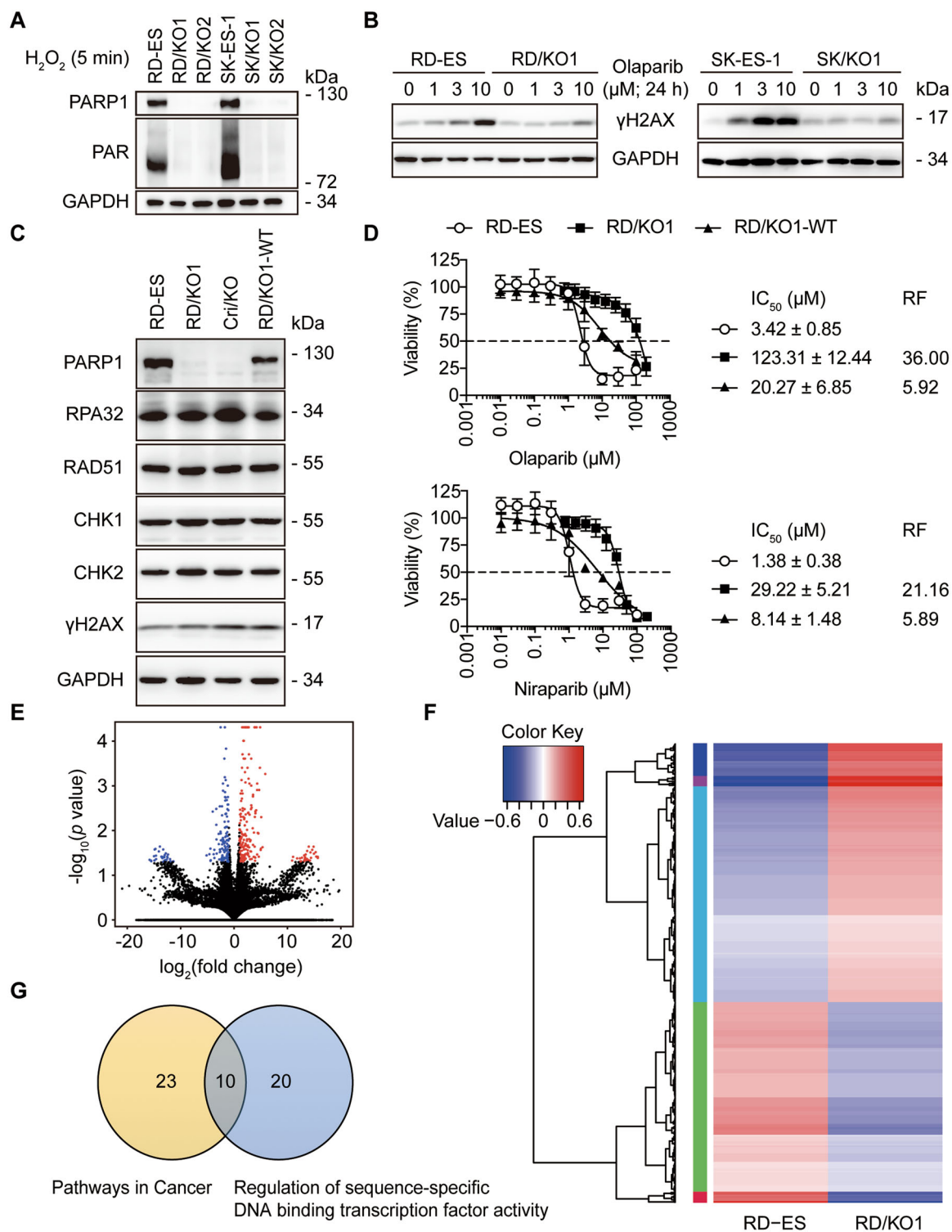


Fig. 1 (See legend on next page.)

(see figure on previous page)

Fig. 1 Characterization of *PARP1*-knockout (KO) (*PARP1*/KO) variants. **a** Levels of PARP1 and PAR were detected by western blotting in different *PARP1*/KO variants (KO1 and KO2) of RD-ES and SK-ES-1 cells exposed to 200 μ M H₂O₂ for 5 min. **b** Accumulation of γ H2AX was reduced in *PARP1*/KO cells relative to parental cells treated with olaparib (0, 1, 3, or 10 μ M). **c** Levels of DNA repair-related proteins in the RD-ES, RD/KO1, Cri/KO, and RD/KO1-WT cells were determined by western blotting. **d** Changes in PARPi sensitivity in response to *PARP1* loss and *PARP1* reconstitution. IC₅₀ values from three independent experiments were expressed as mean \pm SD. Error bars represent the SD. The resistance factor (RF) is the ratio of the averaged IC₅₀ value of indicated PARPi in given cells to that of the same PARPi in RD-ES cells. **e** Volcano plots of the differentially expressed genes in RD/KO1 cells [\log_2 fold change >1 with statistical significance ($p < 0.05$)] detected by RNA-seq. Significantly upregulated and downregulated genes were colored in red and blue, respectively. X axis: \log_2 fold change of gene expression. Y axis: statistical significance of the differential expression in the scale of $-\log_{10}$ (p value). **f** Hierarchical clustered heatmap of differentially expressed genes in *PARP1* loss cells: rows represent cell lines and columns represent genes. Genes with similar expression patterns are within the same cluster and close to each other, and they may have similar functions or participate in the same biological processes. In clustering analysis, high expression and low expression genes are colored in red and blue, respectively (Genes were shown in Supplementary Table S1 from top to bottom). **g** Differentially expressed genes in RD/KO1 cells involved in “pathways in cancer” and “regulation of sequence-specific DNA binding transcription factor activity” were plotted in a Venn diagram to display commonly affected genes (Genes were shown in Supplementary Table S2).

Table S1), while RT-qPCR showed 2.7–6.8-fold increases in *PARP1*-KO Ewing sarcoma RD/KO1, Cri/KO and SK/KO1 cells and pancreatic CAPAN1/KO cells (Fig. 2c, left). Similar increases in FoxO1 protein levels were observed in these cells (Fig. 2c, middle and right). Notably, *PARP1* complementation could reduce, though not eliminate, the *PARP1* loss-mediated increase in either mRNA or protein levels of this gene (Fig. 2c). To further validate these results, we overexpressed *PARP1* by transfecting GFP-*PARP1* into RD-ES. The result showed that exogenous PARP1 overexpression could reduce endogenous FoxO1 protein levels by 44% (Fig. 2d). These results indicate that PARP1 negatively regulates *FoxO1* gene transcription. Moreover, transcriptional regulation of *FoxO1* by PARP1 is not just limited to Ewing sarcoma cells; similar changes were observed in CAPAN1 cells (Fig. 2c). Furthermore, though *FoxO1* has been reported to be a direct target gene of EWS-FLI1 in Ewing sarcoma cells²¹, this regulation is independent of EWS-FLI1 because it does not exist in CAPAN1 cells.

PARP1 binding to the *FoxO1* promoter

To demonstrate how PARP1 regulates *FoxO1* transcription, we evaluated whether PARP1 binds to the *FoxO1* promoter. To conduct the EMSA assay, we used three FAM-labeled fragments correspondingly located at –753 to –1032 (*FoxO1*-L), –1289 to –1565 (*FoxO1*-M), and –1678 to –1995 (*FoxO1*-R) upstream of the transcription start site (TSS) in the *FoxO1* promoter region as probes (Fig. 3a; the 2 kb promoter region of the human *FoxO1* gene and the location and sequence of *FoxO1*-L, *FoxO1*-M, and *FoxO1*-R were shown in Supplementary Table S3). The result showed a clear probe band in the control group (Lane 1, no PARP1 for each panel in Fig. 3b). As PARP1 was added by increasing amounts of 2 to 10 μ g, the probe band for each group was progressively reduced in size and finally disappeared while more DNA-protein complexes formed (Lanes 2–4; 2, 5, and 10 μ g

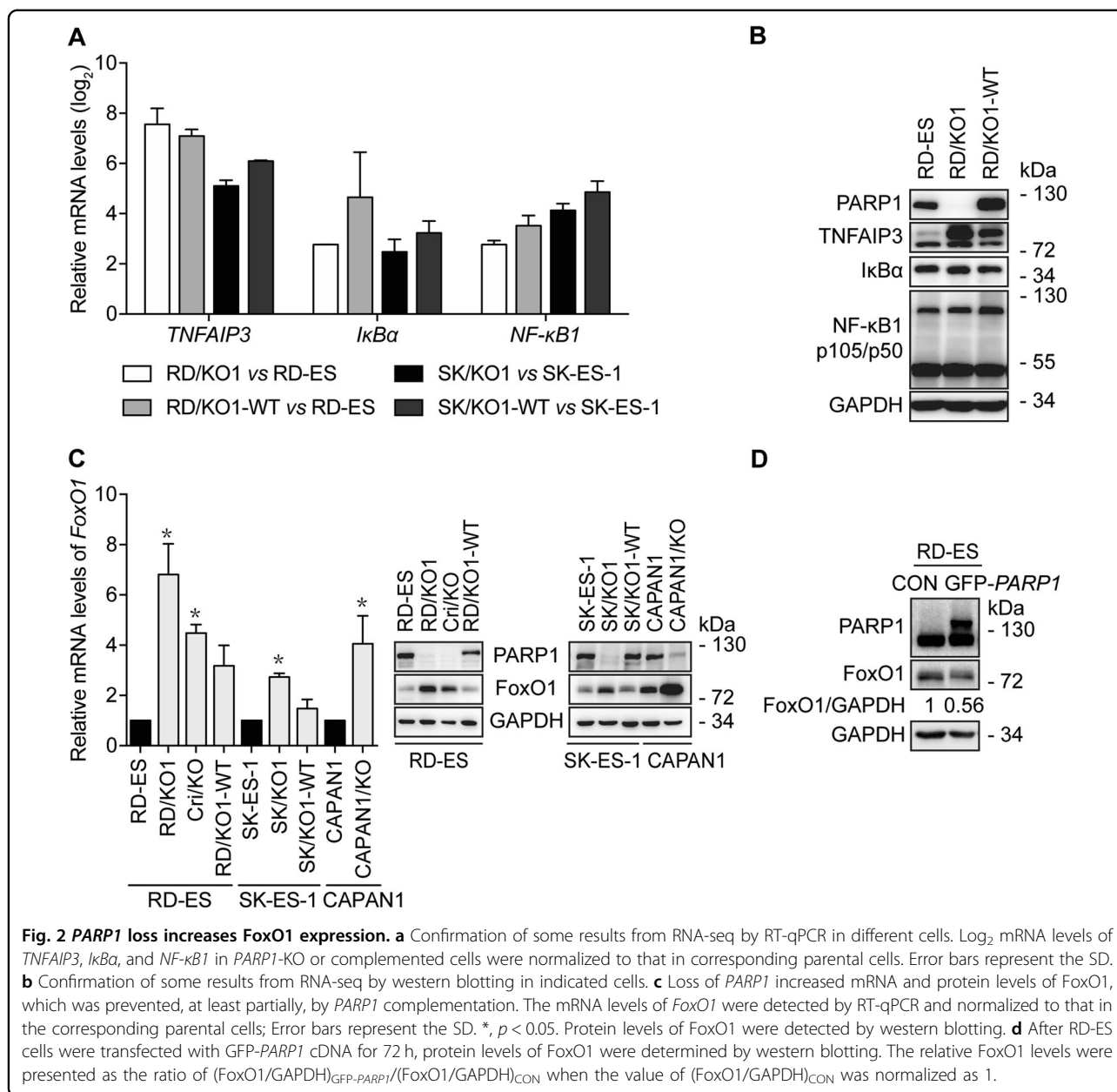
PARP1 for each panel in Fig. 3b). Importantly, adding an excess of 40-fold of unlabeled cold probe DNA partially recovered the probe band and almost completely eliminated FAM-labeled DNA-protein complexes (Lane 5; 10 μ g PARP1 for each panel in Fig. 3b). The results indicate that PARP1 specifically binds to DNA sequences that consist of the *FoxO1* promoter region in the in vitro system.

To confirm the in vitro data, we conducted a ChIP assay using RD-ES, RD/KO1 and RD/KO1-WT cells. The results showed that endogenous PARP1 protein bound to the *FoxO1* promoter at the L, M, and R regions in RD-ES and RD/KO1-WT cells, while PARP1 binding in RD/KO1 cells was comparable to that of IgG in the same regions of the *FoxO1* promoter in all tested cells (Fig. 3c). These data further strengthen the conclusion that PARP1 can specifically bind to the *FoxO1* promoter.

To more accurately define the DNA sequences to which PARP1 binds in the *FoxO1* promoter, we performed DNase I footprinting assays with purified PARP1 protein and DNA fragments (L, M, and R) corresponding to the *FoxO1* promoter. The results showed that 30 μ g PARP1 produced stronger protection against the DNase I-mediated degradation of L and R than M [Fig. 3d (the indicated sequences) and Supplementary Figure S1]. Two regions (denoted as *FoxO1*-L-B and *FoxO1*-R-B) that seemed to be protected were located at –813 bp to –826 bp and –1805 bp to –1828 bp on the *FoxO1* promoter (Fig. 3d). The results indicate that PARP1 is likely to bind to the *FoxO1* promoter *via* these two regions and regulate *FoxO1* transcription.

The binding of PARP1 to the *FoxO1* promoter is sequence-specific

As a DNA repair factor, PARP1 binds to single or double-strand broken DNA without any apparent sequence preference^{22,23}. To demonstrate whether PARP1 binding to the *FoxO1* promoter has sequence specificity,



we used probes containing *FoxO1-L-B* and *FoxO1-R-B* and their respective mutants containing three or four point mutations (Fig. 4a) as probes in an EMSA assay. Data showed that these point mutations did not cause detectable changes in PARP1 binding to the probe DNA (Lane 3 vs Lane 2 and Lane 6 vs Lane 5 in Fig. 4b). In contrast, complete deletions of *FoxO1-L-B* and *FoxO1-R-B* (Fig. 4a) increased unbound probes (Lane 3 vs Lane 2 and Lane 6 vs Lane 5 in Fig. 4c) probably due to PARP1 binding to the probe DNA. However, these deletions did not fully restore unbound probes to control levels (Lane 3 vs Lane 1 and Lane 6 vs Lane 1 in Fig. 4c), revealing PARP1 non-specific binding, probably because the probes

had 2 ends comparable to broken DNA. Nevertheless, the results reveal that PARP1 indeed binds to the *FoxO1* promoter at the -813 to -826 bp (*FoxO1-L-B*) and -1805 to -1828 bp (*FoxO1-R-B*) regions in a sequence-specific manner.

Our conclusion was further supported by data from a novel DNA pulldown assay termed FREP that was done to minimize detectable non-specific PARP1 binding through restriction enzyme digestion²⁴. To do this assay, the 3' free end of the DNA was cleaved off by EcoR I and the single-stranded DNA that was not cleaved off with BamH I was therefore discarded along with the bead (Fig. 4d). *FoxO1-L-B* and *FoxO1-R-B* were used as corresponding

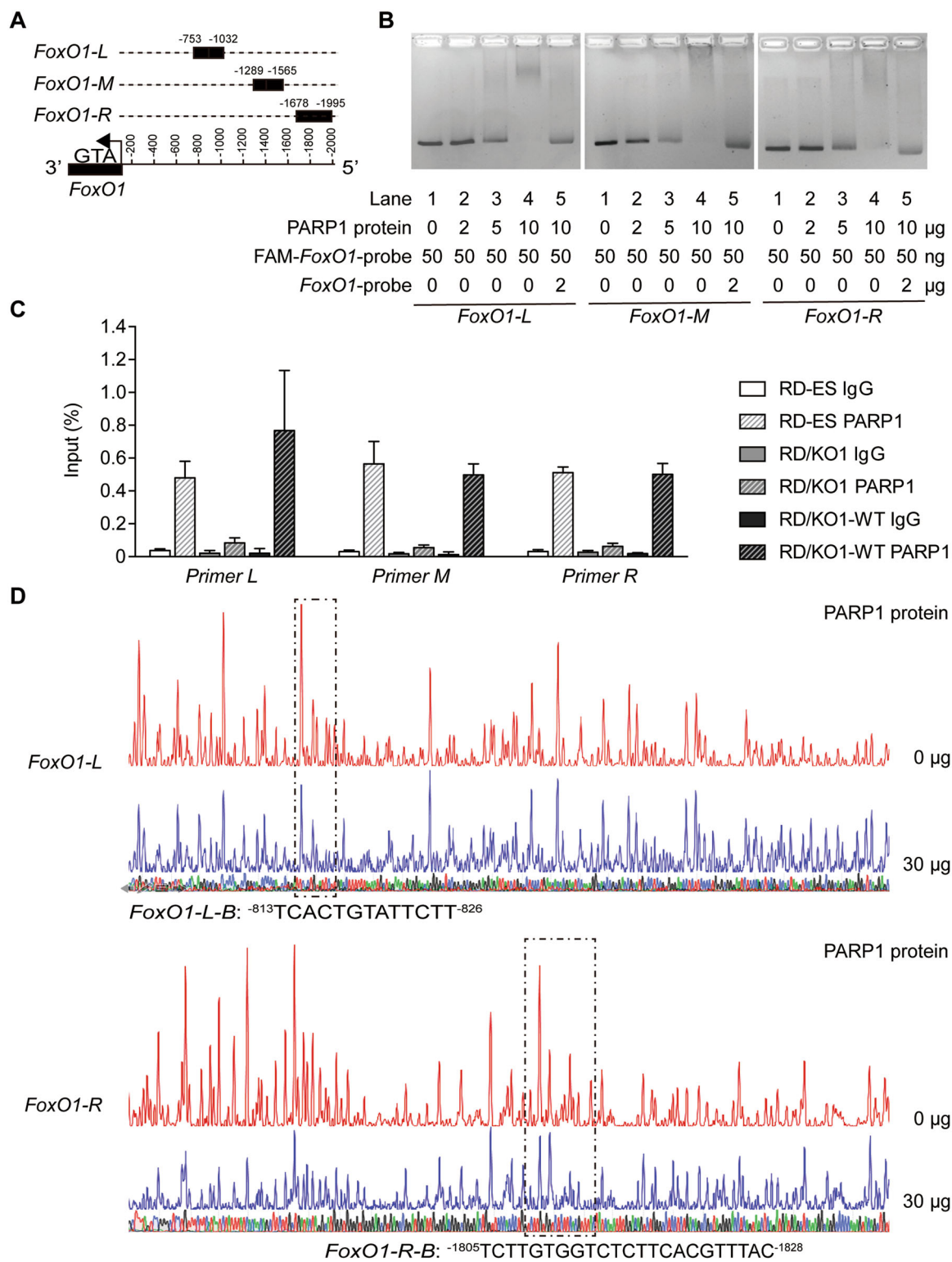


Fig. 3 (See legend on next page.)

(see figure on previous page)

Fig. 3 PARP1 binding to particular regions on the *FoxO1* promoter. **a** Schematic representation of the locations of particular nucleotide fragments (*FoxO1-L*, *-M*, and *-R*) on the *FoxO1* promoter analyzed by EMSA. **b** The binding of purified PARP1 to particular nucleotide fragments (*FoxO1-L*, *-M*, and *-R*) were analyzed by EMSA. For the competition assays, 40-fold excess of unlabeled DNA fragments were added to the reaction mixture before adding FAM-labeled probes, and the labeled PARP1-*FoxO1* complexes were almost completely displaced. **c** RD-ES, RD/KO1, and RD/KO1-WT cells were subjected to ChIP analyses using the antibody against PARP1 and an isotype-matched IgG as a negative control. The association of PARP1 with the *FoxO1* gene promoter was quantified by RT-qPCR using primers targeting *FoxO1-L*, *-M*, and *-R*, respectively. Error bars represent the SD. **d** Identification of PARP1-protected regions on *FoxO1-L* and *FoxO1-R* by DNase I footprinting assays. Electropherograms showed the whole region of the *FoxO1-L/R* after digestion with DNase I following incubation in the presence (blue) or absence (red) of PARP1. The DNA sequences of the PARP1-protected regions were marked with dashed rectangles and denoted as *FoxO1-L-B* (⁻⁸¹³TCACTGTATTCTT⁻⁸²⁶) and *FoxO1-R-B* (⁻¹⁸⁰⁵TCTTGGTCTCTTCACGTTTAC⁻¹⁸²⁸).

competitors of the biotin-labeled *FoxO1-L-B* and *FoxO1-R-B*, while a non-specific 31 bp DNA sequence (*NS*) labeled with biotin was used as the control for non-specific PARP1 binding. The PARP1-DNA complexes digested with EcoR I and BamH I were detected by western blotting with an anti-PARP1 antibody. Results (Fig. 4e) revealed that PARP1 bound to the biotin-labeled *FoxO1-L-B* (Lane 3) and *FoxO1-R-B* (Lane 6) much more than the control (Lane 9). Importantly, PARP1 bound to biotin-labeled *FoxO1-L-B* and *FoxO1-R-B* was largely competed away by free *FoxO1-L-B* and *FoxO1-R-B*, respectively (Lane 4 and 7, Fig. 4e). Therefore, these data further indicate that PARP1 sequence-specific binding to the *FoxO1* promoter inhibits *FoxO1* transcription.

PARP1 transcriptional regulation of *FoxO1* is independent of its catalytic activity

PARP1 has been shown to regulate gene transcription in two modes independent of or dependent on its catalytic activity¹⁵. To test whether its poly(ADP-ribose) polymerase activity is required for its transcriptional regulation on *FoxO1*, we treated RD-ES and SK-ES-1 cells with the PARPi olaparib. Olaparib inhibits the PARP1 enzymatic activity but does not affect PARP1 expression^{3,25}. The treatments with olaparib did not cause obvious changes in mRNA or protein levels of *FoxO1* (Fig. 5a and Supplementary Fig. S2). To verify this result, we used a catalytic mutant of PARP1 by replacing the glutamic acid residue at 988 with a lysine residue (E988K) to complement RD/KO1 (resulting cells, RD/KO1-E988K)⁴. E988K has no poly(ADP-ribose) polymerase activity but keeps the mono-ADP-ribosyl-transferase activity⁴. The expression of E988K in RD-ES/KO1 cells led to apparent decreases in *FoxO1* mRNA and protein levels (Fig. 5b, c). These results further indicate that transcriptional regulation of *FoxO1* by PARP1 is independent of its catalytic activity.

FoxO1 does not contribute to the sensitivity of RD-ES cells to PARP inhibitors

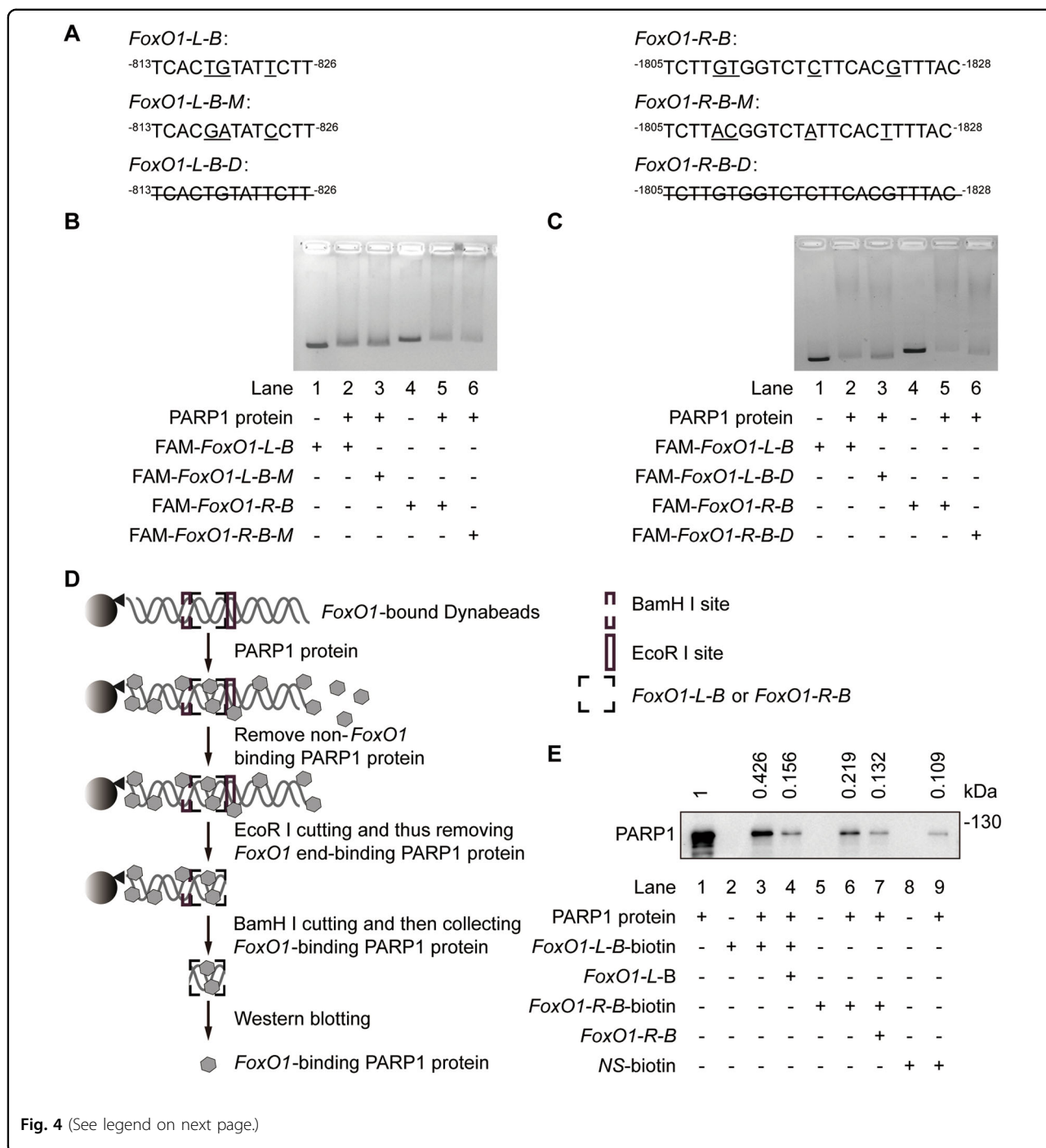
We further evaluated the effects of PARP1 loss and reconstitution on the target genes of the transcription factor FoxO1. The data revealed that loss and exogenous

re-expression of *PARP1* in RD-ES cells caused similar significant changes in mRNA levels of *FoxO1* and *p21*, one of the target genes of FoxO1²⁶. However, only marginal changes took place in mRNA levels of *PUMA* and *Bim*, the other two target genes of FoxO1²⁷ (Fig. 5d).

We demonstrate that *PARP1* loss leads to FoxO1 overexpression and cellular resistance to PARP inhibitors. Therefore, we further investigated whether FoxO1 overexpression contributed to PARPi resistance. We established a FoxO1-overexpressed model by transfecting GFP-*FoxO1* into RD-ES cells that normally express PARP1 protein. FoxO1 overexpression was verified in Fig. 5e. However, FoxO1 overexpression did not change the cellular sensitivity of PARPis olaparib, niraparib, or talazoparib (Fig. 5f), indicating that there is no correlation between FoxO1 expression and the sensitivity of RD-ES cells to PARPis.

FoxO1 has been shown to regulate cellular sensitivity to several DNA damaging agents²⁸. We thus evaluated the changes in the mRNA levels of *FoxO1* and its target genes in RD-ES cells exposed to cisplatin, carmustine, and temozolomide. As shown in Fig. 5g, only carmustine increased the mRNA levels of *FoxO1* at its high concentration. Notably, changes in the mRNA levels of *p21*, *PUMA*, and *Bim* were different in response to different treatments.

Then we tested the sensitivity of RD-ES, RD/KO1, and *FoxO1*-overexpressed RD-ES (RD-ES FoxO1 OE) (Fig. 5h) cells to cisplatin, carmustine, and temozolomide. The results suggested that the decreased sensitivity of RD/KO1 cells to cisplatin was probably not caused by increased FoxO1 expression. In contrast, the sensitivity of both RD/KO1 and RD-ES FoxO1 OE cells to carmustine significantly increased while the sensitivity of these cells to temozolomide basically kept unchanged relative to that of RD-ES cells (Fig. 5i). Carmustine but not the other two alkylating agents showed some dependency on FoxO1 in its killing RD-ES, which was consistent with the fact that cisplatin and temozolomide did not cause significant changes in the mRNA levels of *FoxO1* while carmustine could significantly increase the mRNA levels of *FoxO1* at 50 μ M (Fig. 5g).



Discussion

Recent studies on PARP1 have been largely focused on its functions in DNA repair, primarily due to the successful clinical uses of PARPis. This may be a reason why our understanding on PARP1 transcriptional regulation has been less established. In this study, we investigated PARP1-mediated gene transcription by using *PARP1*-KO cells which did not respond to PARPi treatments. *FoxO1*,

encoding a transcription factor, was up-regulated in its mRNA and protein levels in the *PARP1*-KO Ewing sarcoma RD/KO1, Cri/KO, and SK/KO1 cells and pancreatic cancer CAPAN1/KO cells. Importantly, *PARP1* complementation prevented *PARP1* loss-mediated increase in its mRNA or protein levels, though partly in some cells. The results indicate that PARP1 represses *FoxO1* gene transcription. We subsequently demonstrated that

(see figure on previous page)

Fig. 4 PARP1 binding to the specific DNA sequences on the *FoxO1* promoter. **a** The FAM-labeled probes containing sequences of *FoxO1-L-B* (left) and *FoxO1-R-B* (right) and corresponding mutated probes (underlined; *FoxO1-L-B-M* and *FoxO1-R-B-M*), and the deleted sequences (line-through; *FoxO1-L-B-D* and *FoxO1-R-B-D*). **b** EMSA was carried out using normal or mutated FAM-labeled probes. The amount of DNA-protein complexes detected in FAM-labeled mutant probes was similar to that in FAM-labeled normal probes. **c** EMSA was carried out using FAM-labeled normal and deletion probes. Fewer DNA-protein complexes were detected with FAM-labeled deletion probes than the FAM-labeled normal probes followed by PARP1 incubation. **d** Schematic representation of the flanking restriction enhanced pulldown (FREP). A biotinylated DNA fragment is conjugated to streptavidin-coated magnetic Dynabeads (Invitrogen, Carlsbad, CA). This fragment is engineered to include the *FoxO1-L-B* or *FoxO1-R-B* specific ("bait") sequence (black dashed box), flanked by restriction enzyme cleavage sites for BamH I proximally (gray dashed box) and EcoR I distally (gray box). DNA-beads are mixed with PARP1 protein. A free non-biotinylated *FoxO1-L-B* or *FoxO1-R-B* DNA fragment can be included in the control reaction at this stage as a specific competitor. Magnetic separation and wash remove non-DNA binding PARP1 protein. EcoR I digestion releases 3' DNA end-binding PARP1, and BamH I digestion separates the sequence-specific *FoxO1-L-B* or *FoxO1-R-B* binding PARP1 from the 5' DNA and Dynabeads. Western blotting identifies PARP1 binding to *FoxO1-L-B* or *FoxO1-R-B*. **e** The PARP1-DNA complexes cut with EcoR I and BamH I were detected by western blotting. The relative levels of *FoxO1*-bound PARP1 were presented as the ratio of *FoxO1*-bound PARP1 band intensity/PARP1 input band intensity when the value of PARP1 input band intensity was normalized as 1. Lane 1: PARP1 inputs, lane 2: labeled *FoxO1-L-B*-beads, lane 3: PARP1 with labeled *FoxO1-L-B*-beads, lane 4: PARP1 with labeled *FoxO1-L-B*-beads and cold competitor (40-fold excess of free *FoxO1-L-B*-beads), lane 5: labeled *FoxO1-R-B*-beads, lane 6: PARP1 with labeled *FoxO1-R-B*-beads, lane 7: PARP1 with labeled *FoxO1-R-B*-beads and cold competitor (40-fold excess of free *FoxO1-R-B*-beads), lane 8: a labeled non-specific DNA sequence (NS-beads) and lane 9: PARP1 with labeled NS-beads.

PARP1 specifically bound to the *FoxO1* promoter. It was also revealed that regions of -813 to -826 bp (i.e., 5'-TCACTGTATTCTT-3') and -1805 to -1828 bp (i.e., 5'-TCTTGTGGTCTCTTCACGTTTAC-3') upstream of the TSS on the *FoxO1* promoter were required for this binding, indicating its DNA sequence dependency or specificity. Moreover, negative transcriptional regulation of *FoxO1* by PARP1 was independent of its enzymatic activity. This may be why *FoxO1* expression is not correlated with cellular PARPi sensitivity because almost all the present PARPis are enzymatic inhibitors. Nevertheless, our data suggest a possible correlation of the transcriptional regulation of *FoxO1* by PARP1 with the carmustine sensitivity in RD-ES cells. This provides a direction for our future exploration.

As a DNA repair factor, PARP1 can bind to DNA in a DNA sequence-independent manner, and inhibition of its enzymatic activity increases this binding^{4,23,29}. In striking contrast, when functioning as a transcriptional regulation factor, the binding of PARP1 to gene promoter regions requires particular DNA sequences. For example, PARP1 was shown to bind to the 5'-GTTTCACAAT-3' sequence in the *BRCA2* promoter¹⁴, to the 5'-GCTGTGGGAA-3' sequence in the *Tcirg1* promoter²⁹, to the 5'-ATGGTctACCTA-3' sequence in the *HFE* promoter³⁰, to the 5'-GTTG-3' sequence in the *CXCL1* promoter³¹, and to the 5'-TGTTG-3' sequence in the *cTnT* promoter³². The PARP1 binding results in negative transcriptional regulation of the former three genes but positive regulation of the latter two. Different from only a single-nucleotide sequence motif that is required for the PARP1 binding in these studies^{14,29-32}, our data reveal that two specific motifs (i.e., 5'-TCACTGTATTCTT-3' and 5'-TCTTGTGGTCTCTTCACGTTTAC-3') are needed for *FoxO1*

transcriptional inhibition. The two motifs are separately located at the regions at a distance of 979 bp on the *FoxO1* promoter. This is a new PARP1-gene promoter binding mode. Notably, the 5'-TG-3' nucleotide sequence appears in the above mentioned PARP1 binding motifs (except *BRCA2*). However, this sequence might not be a critical consensus nucleotide sequence for the PARP1-gene promoter binding because our result revealed that the mutation of 5'-TG-3' did not change the PARP1 binding. Therefore, previous studies and our own indicate that transcriptional regulation by PARP1, at least by way of nucleotide-sequence-dependent binding to the gene promoter, is gene specific in the aspects of PARP1-bound DNA sequence(s), transcriptional inhibition or stimulation and PARP1-polymerase dependency. At present, the issues on this specificity remain to be explored, particularly including what the determining factors are, whether any other cofactors are involved, and which domain(s) of PARP1 contribute to specific binding.

The transcription factor FoxO1 is a member of the FoxO family and regulates diverse gene expression in controlling various biological processes such as tumorigenesis and aging³³. FoxO1 can function as a tumor suppressor. On the one hand, FoxO1 inhibits cancer cell proliferation by activating the transcription of *p21*, encoding a cell cycle inhibitor²⁶; on the other, FoxO1 induces apoptosis by upregulating expression of several pro-apoptotic factors including *PUMA* and *Bim*^{26,34}. Moreover, FoxO1 also affects cellular sensitivity or resistance to anticancer drugs^{26,28,34-36}. Though its post-transcriptional modifications and its transcriptional control of target genes have been extensively investigated³⁷, relatively little is known about transcriptional regulation of the *FoxO1* gene itself. Our current study reveals that

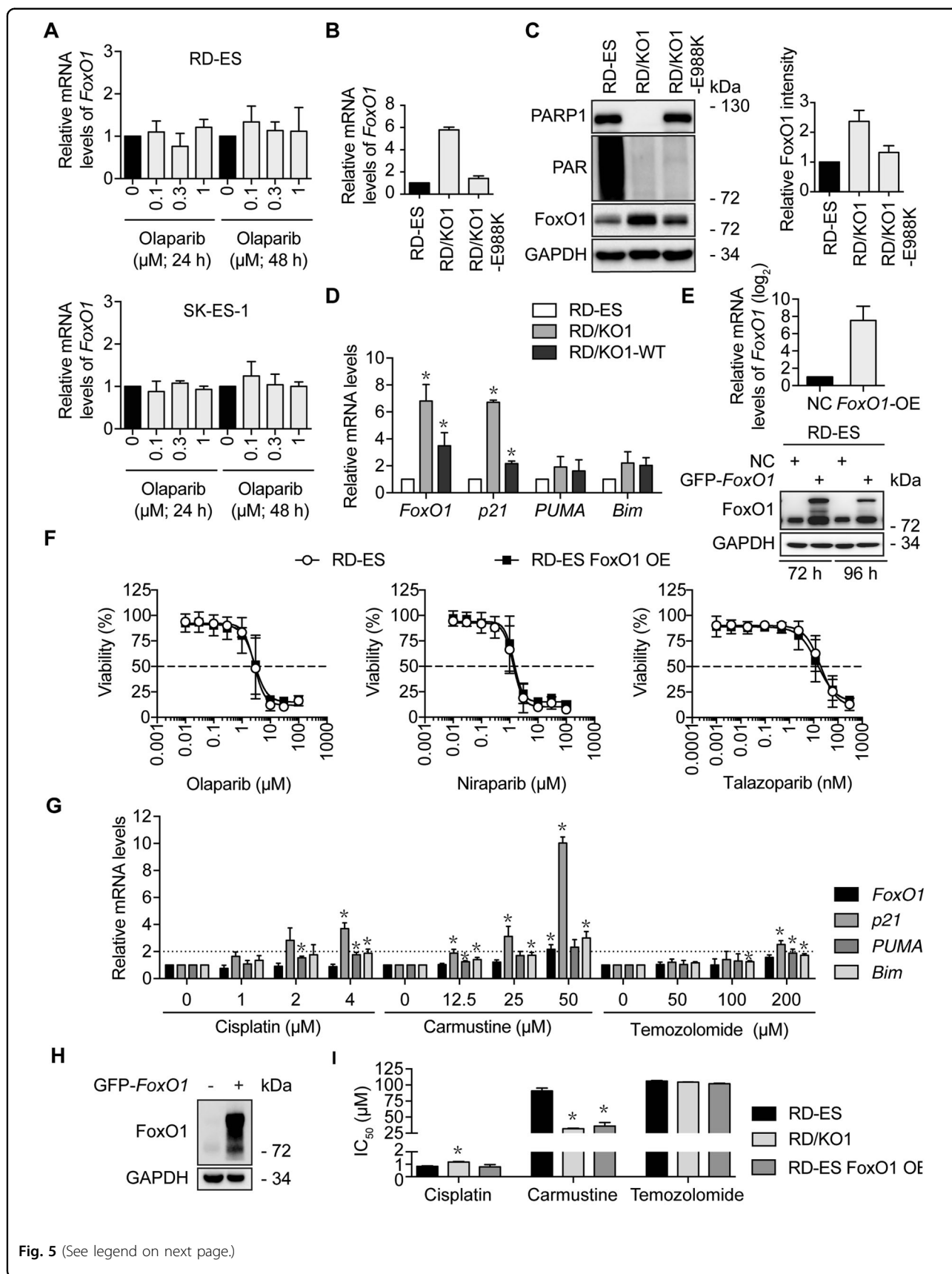


Fig. 5 (See legend on next page.)

(see figure on previous page)

Fig. 5 The expression of *FoxO1* regulated by PARP1 is independent of its catalytic activity and *FoxO1* does not affect the sensitivity of RD-ES cells to PARP inhibitors. **a** RD-ES (upper) and SK-ES-1 (lower) cells were incubated in the indicated concentrations of olaparib for 24 h or 48 h. Then, mRNA levels of *FoxO1* were detected by RT-qPCR. **b** mRNA levels of *FoxO1* in RD/KO1 cells and their stably-transfected with mutated-*PARP1* cDNA (E988K) variants were detected by RT-qPCR. **c** Protein levels of *FoxO1* in RD/KO1 cells and their stably-transfected with mutated-*PARP1* cDNA (E988K) variants were detected by western blotting. The relative *FoxO1* levels were presented as the ratio of $(\text{FoxO1}/\text{GAPDH})_{\text{KO1 or E988K}}/(\text{FoxO1}/\text{GAPDH})_{\text{RD-ES}}$ when the value of $(\text{FoxO1}/\text{GAPDH})_{\text{RD-ES}}$ was normalized as 1. Data were expressed as mean \pm SD from three independent experiments. **d** Effects of *PARP1* loss and *PARP1* reconstitution on the expression of *FoxO1* target genes. mRNA levels were detected by RT-qPCR. *, $p < 0.05$. **e** RD-ES cells were transfected with GFP-*FoxO1* cDNA for 72 h and 96 h, and the mRNA (left) and protein (right) levels of *FoxO1* were detected by RT-qPCR and western blotting, respectively. **f** Survival curves of olaparib, niraparib and talazoparib-treated RD-ES and *FoxO1*-overexpressed RD-ES (RD-ES *FoxO1* OE) cells assessed by CCK-8 assays. Error bars represent the SD. **g** Changes of the mRNA levels of *FoxO1* and its target genes. RD-ES cells were treated with cisplatin, carmustine and temozolomide for 12 h. Then, mRNA levels of *FoxO1*, *p21*, *PUMA* and *Bim* were detected by RT-qPCR and normalized to those in RD-ES cells without any treatments. *, $p < 0.05$. **h** *FoxO1* overexpression by transfecting GFP-*FoxO1* into RD-ES cells was determined by western blotting. **i** Sensitivity of RD-ES, RD/KO1 and RD-ES *FoxO1* OE cells to cisplatin, carmustine and temozolomide. Cells were exposed to gradient concentrations of the tested agents for 72 h. IC_{50} values from three independent experiments were expressed as mean \pm SD. Error bars represent the SD. *, $p < 0.05$.

PARP1 binds to the *FoxO1* promoter and represses *FoxO1* expression, which is independent of PARP1 enzymatic activity. Knockout and complementation of *PARP1* separately caused a consistent increase and reduction in both mRNA and protein levels of *FoxO1*. Notably, cells that normally express PARP1 and that are complemented with *PARP1* (WT or mutated) have low levels of *FoxO1* expression. Therefore, PARP1 binding appears not to affect the basal expression of the *FoxO1* gene. This conclusion might be supported also by the finding that in HEK293T cells transfected with both FLAG-*PARP1* and HA-*FoxO1*, both proteins can be detected at the same time³⁸. Therefore, in addition to transcription factors E2F-1³⁹, FoxC1⁴⁰, FoxO3⁴¹, and EWS-FLI1²¹, PARP1 is another new transcriptional regulator of the *FoxO1* gene by direct binding to its promoter.

Collectively, this study demonstrates a new PARP1-gene promoter binding mode evidenced by direct PARP1 binding to two separate motifs on the *FoxO1* promoter. PARP1 is a new transcriptional repressor of *FoxO1*, encoding an important transcription factor with extensive biological functions. The regulation of *FoxO1* expression by PARP1 is independent of its polymerase activity and cellular PARP1 sensitivity. These findings provide new insights into both PARP1 functions and *FoxO1* transcriptional regulation, helping to further understand the roles of PARP1 and *FoxO1* in tumorigenesis and cancer therapy.

Materials and methods

Details about drugs and antibodies, cell culture, stable KO of PARP1 with the CRISPR/Cas9 technique, RNA sequencing (RNA-seq), quantitative real-time polymerase chain reaction (RT-qPCR), EMSA and competitive binding assays, ChIP, DNase I footprinting assays, and FREP are provided in Supplementary Materials and Methods.

Western blotting

Standard western blotting⁴² was used to detect the changes in protein levels caused by the indicated treatments.

Cytotoxicity assays

Cell Counting Kit 8 (CCK-8, Dojindo Laboratories, Kumamoto, Japan) assays were used to detect cytotoxicity as previously described⁴³.

Plasmid construction, PARP1 protein purification, generation of cells expressing PARP1 or its mutants

Plasmid construction, PARP1 protein purification, generation of cells expressing PARP1, or its mutants were conducted as previously reported⁴.

Statistical analysis

All data were representative of three independent experiments. Data were presented as mean \pm SD (standard deviation), and no data was excluded from analysis. A Student's *t* test (two-tailed) was used to compare two groups. Only $p < 0.05$ was considered statistically significant.

Acknowledgements

This work was supported by grants from the National Natural Science Foundation of China (81573450 and 81773764), the Chinese Academy of Sciences (XDA12020104, XDA12020109 and CASIMM0120185003), the Nova Development Program of the Shanghai Institute of *Materia Medica*, the Science and Technology Commission of Shanghai Municipality (19ZR1467900), the State Key Laboratory of Drug Research and the Open Studio for Drugability Research of Marine Natural Products in the Qingdao National Laboratory for Marine Science and Technology.

Author details

¹Division of Anti-Tumor Pharmacology, State Key Laboratory of Drug Research, Shanghai Institute of *Materia Medica*, Chinese Academy of Sciences, Shanghai 201203, China. ²University of Chinese Academy of Sciences, No.19A Yuquan Road, Beijing 100049, China. ³Open Studio for Drugability Research of Marine Natural Products, Pilot National Laboratory for Marine Science and Technology, Qingdao, Shandong 266237, China

Conflict of interest

The authors declare that they have no conflict of interest.

Publisher's note

Springer Nature remains neutral with regard to jurisdictional claims in published maps and institutional affiliations.

Supplementary Information accompanies this paper at (<https://doi.org/10.1038/s41419-020-2265-y>).

Received: 3 September 2019 Revised: 9 January 2020 Accepted: 9 January 2020

Published online: 28 January 2020

References

- Ding, J., Miao, Z. H., Meng, L. H. & Geng, M. Y. Emerging cancer therapeutic opportunities target DNA-repair systems. *Trends Pharmacol. Sci.* **27**, 338–344 (2006).
- He, J. X., Yang, C. H. & Miao, Z. H. Poly(ADP-ribose) polymerase inhibitors as promising cancer therapeutics. *Acta Pharmacol. Sin.* **31**, 1172–1180 (2010).
- Wang, Y. Q. et al. An update on poly(ADP-ribose)polymerase-1 (PARP-1) inhibitors: opportunities and challenges in cancer therapy. *J. Med. Chem.* **59**, 9575–9598 (2016).
- Chen, H. D. et al. Increased PARP1-DNA binding due to autoPARylation inhibition of PARP1 on DNA rather than PARP1-DNA trapping is correlated with PARP1 inhibitor's cytotoxicity. *Int. J. Cancer* **145**, 714–727 (2019).
- Yuan, B. et al. Poly(ADP-ribose)polymerase (PARP) inhibition and anticancer activity of simiparib, a new inhibitor undergoing clinical trials. *Cancer Lett.* **386**, 47–56 (2017).
- He, J. X. et al. Novel PARP1/2 inhibitor mefuparib hydrochloride elicits potent in vitro and in vivo anticancer activity, characteristic of high tissue distribution. *Oncotarget* **8**, 4156–4168 (2017).
- Ye, N. et al. Design, synthesis, and biological evaluation of a series of benzo[de][1,7]naphthyridin-7(8H)-ones bearing a functionalized longer chain appendage as novel PARP1 inhibitors. *J. Med. Chem.* **56**, 2885–2903 (2013).
- Chen, J. Y. et al. Synthesis of isoquinolinone-based tricycles as novel poly(ADP-ribose) polymerase-1 (PARP-1) inhibitors. *Bioorg. Med. Chem. Lett.* **24**, 2669–2673 (2014).
- Chen, X. X. et al. Design and synthesis of 2-(4,5,6,7-tetrahydrothienopyridin-2-yl)-benzimidazole carboxamides as novel orally efficacious Poly(ADP-ribose) polymerase (PARP) inhibitors. *Eur. J. Med. Chem.* **145**, 389–403 (2018).
- Chen, W. H. et al. Discovery of potent 2,4-difluoro-linker poly(ADP-ribose) polymerase 1 inhibitors with enhanced water solubility and in vivo anticancer efficacy. *Acta Pharmacol. Sin.* **38**, 1521–1532 (2017).
- Chen, W. H. et al. Discovery, mechanism and metabolism studies of 2,3-difluorophenyl-linker-containing PARP1 inhibitors with enhanced in vivo efficacy for cancer therapy. *Eur. J. Med. Chem.* **138**, 514–531 (2017).
- Wang, Y. T. et al. Acquired resistance of phosphatase and tensin homolog-deficient cells to poly(ADP-ribose) polymerase inhibitor and Ara-C mediated by 53BP1 loss and SAMHD1 overexpression. *Cancer Sci.* **109**, 821–831 (2018).
- Yang, Z. M. et al. Combining 53BP1 with BRCA1 as a biomarker to predict the sensitivity of poly(ADP-ribose) polymerase (PARP) inhibitors. *Acta Pharmacol. Sin.* **38**, 1038–1047 (2017).
- Wang, J. H. et al. Poly(ADP-ribose) polymerase-1 down-regulates BRCA2 expression through the BRCA2 promoter. *J. Biol. Chem.* **283**, 36249–36256 (2008).
- Schiewer, M. J. & Knudsen, K. E. Transcriptional roles of PARP1 in cancer. *Mol. Cancer Res.* **12**, 1069–1080 (2014).
- Kraus, W. L. & Hottiger, M. O. PARP-1 and gene regulation: progress and puzzles. *Mol. Asp. Med.* **34**, 1109–1123 (2013).
- Schiewer, M. J. et al. Dual roles of PARP-1 promote cancer growth and progression. *Cancer Discov.* **2**, 1134–1149 (2012).
- Frizzell, K. M. et al. Global analysis of transcriptional regulation by poly(ADP-ribose) polymerase-1 and poly(ADP-ribose) glycohydrolase in MCF-7 human breast cancer cells. *J. Biol. Chem.* **284**, 33926–33938 (2009).
- Ohali, A. et al. Prediction of high risk Ewing's sarcoma by gene expression profiling. *Oncogene* **23**, 8997–9006 (2004).
- Chao, O. S. & Goodman, O. B. Synergistic loss of prostate cancer cell viability by coinhibition of HDAC and PARP. *Mol. Cancer Res.* **12**, 1755–1766 (2014).
- Yang, L., Hu, H. M., Zielinska-Kwiatkowska, A. & Chansky, H. A. FOXO1 is a direct target of EWS-Fli1 oncogenic fusion protein in Ewing's sarcoma cells. *Biochem. Biophys. Res. Commun.* **402**, 129–134 (2010).
- Gradwohl, G. et al. The second zinc-finger domain of poly(ADP-ribose) polymerase determines specificity for single-stranded breaks in DNA. *Proc. Natl Acad. Sci. USA* **87**, 2990–2994 (1990).
- Langelier, M. F. & Pascal, J. M. PARP-1 mechanism for coupling DNA damage detection to poly(ADP-ribose) synthesis. *Curr. Opin. Struct. Biol.* **23**, 134–143 (2013).
- Li, G. et al. The rheumatoid arthritis risk variant CCR6DNP regulates CCR6 via PARP-1. *PLoS Genet.* **12**, e1006292 (2016).
- Kim, G. et al. FDA approval summary: olaparib monotherapy in patients with deleterious germline BRCA-mutated advanced ovarian cancer treated with three or more lines of chemotherapy. *Clin. Cancer Res.* **21**, 4257–4261 (2015).
- Farhan, M. et al. FOXO signaling pathways as therapeutic targets in cancer. *Int. J. Biol. Sci.* **13**, 815–827 (2017).
- Calnan, D. R. & Brunet, A. The FoxO code. *Oncogene* **27**, 2276–2288 (2008).
- Chen, C. et al. FOXO1 associated with sensitivity to chemotherapy drugs and glial-mesenchymal transition in glioma. *J. Cell Biochem.* **120**, 882–893 (2019).
- Beranger, G. E. et al. RANKL treatment releases the negative regulation of the poly(ADP-ribose) polymerase-1 on Tcigr1 gene expression during osteoclastogenesis. *J. Bone Miner. Res.* **21**, 1757–1769 (2006).
- Pelham, C. et al. Regulation of HFE expression by poly(ADP-ribose) polymerase-1 (PARP1) through an inverted repeat DNA sequence in the distal promoter. *Biochim. Biophys. Acta* **1829**, 1257–1265 (2013).
- Nirodi, C. et al. A role for poly(ADP-ribose) polymerase in the transcriptional regulation of the melanoma growth stimulatory activity (CXCL1) gene expression. *J. Biol. Chem.* **276**, 9366–9374 (2001).
- Huang, K. et al. Analysis of nucleotide sequence-dependent DNA binding of poly(ADP-ribose) polymerase in a purified system. *Biochemistry* **43**, 217–223 (2004).
- Coomans de Brachene, A. & Demoulin, J. B. FOXO transcription factors in cancer development and therapy. *Cell. Mol. Life Sci.* **73**, 1159–1172 (2016).
- Hornsveld, M., Dansen, T. B., Derksen, P. W. & Burgering, B. M. T. Re-evaluating the role of FOXOs in cancer. *Semin. Cancer Biol.* **50**, 90–100 (2018).
- Gao, J. et al. The involvement of FoxO in cell survival and chemosensitivity mediated by Mirk/Dyrk1B in ovarian cancer. *Int. J. Oncol.* **40**, 1203–1209 (2012).
- Beretta, G. L., Corno, C., Zaffaroni, N. & Perego, P. Role of FoxO proteins in cellular response to antitumor agents. *Cancers* **11**, 90 (2019).
- Xing, Y. Q. et al. The regulation of FOXO1 and its role in disease progression. *Life Sci.* **193**, 124–131 (2018).
- Sakamaki, J., Daitoku, H., Yoshimochi, K., Miwa, M. & Fukamizu, A. Regulation of FOXO1-mediated transcription and cell proliferation by PARP-1. *Biochem. Biophys. Res. Commun.* **382**, 497–502 (2009).
- Nowak, K., Killmer, K., Gessner, C. & Lutz, W. E2F-1 regulates expression of FOXO1 and FOXO3a. *Biochim. Biophys. Acta* **1769**, 244–252 (2007).
- Berry, F. B. et al. FOXO1 is required for cell viability and resistance to oxidative stress in the eye through the transcriptional regulation of FOXO1A. *Hum. Mol. Genet.* **17**, 490–505 (2008).
- Essaghir, A., Dif, N., Marbehant, C. Y., Coffey, P. J. & Demoulin, J. B. The transcription of FOXO genes is stimulated by FOXO3 and repressed by growth factors. *J. Bacteriol.* **284**, 10334–10342 (2009).
- Yi, J. M. et al. Triptolide induces cell killing in multidrug-resistant tumor cells via CDK7/RPB1 rather than XPB or p44. *Mol. Cancer Ther.* **15**, 1495–1503 (2016).
- Wang, W. et al. MCL-1 degradation mediated by JNK activation via MEK1/TAK1-MKK4 contributes to anticancer activity of new tubulin inhibitor MT189. *Mol. Cancer Ther.* **13**, 1480–1491 (2014).